REPORT DOCUMENTATION PAGE

AFRL-SR-AR-TR-05-

0517

1. AGENCY USE ONLY *(Leave blank)*	2. REPORT DATE	3. REPORT TYPE AND DATES COVERED
		01 MAY 2003 - 30 SEP 2005 FINAL

4. TITLE AND SUBTITLE
LASER COOLING WITH ULTRAFAST PULSE TRAINS

5. FUNDING NUMBERS
61102F
2301/DX

6. AUTHOR(S)
DR KAERTNER

7. PERFORMING ORGANIZATION NAME(S) AND ADDRESS(ES)
MASSACHUSETTS INSTITUTE OF TECHNOLOGY
77 MASSACHUSETTS AVENUE
CAMBRIDGE MA 02139

8. PERFORMING ORGANIZATION REPORT NUMBER

9. SPONSORING/MONITORING AGENCY NAME(S) AND ADDRESS(ES)
AFOSR/NE
4015 WILSON BLVD
SUITE 713
ARLINGTON VA 22203

10. SPONSORING/MONITORING AGENCY REPORT NUMBER
F49620-03-1-0313

11. SUPPLEMENTARY NOTES

12a. DISTRIBUTION AVAILABILITY STATEMENT
DISTRIBUTION STATEMENT A: Unlimited

12b. DISTRIBUTION CODE

13. ABSTRACT *(Maximum 200 words)*

We have made significant progress toward a demonstration of mode-locked laser cooling using trapped Yb+ ions. We have constructed a Yb+ ion trap system and successfully trapped and laser-cooled clouds of Yb+ ions. We have also constructed and frequency-stabilized a high-repetition-rate mode-locked laser appropriate for demonstrating the cooling technique. We searched for the two-photon transition.

20060111 002

14. SUBJECT TERMS			15. NUMBER OF PAGES
			16. PRICE CODE
17. SECURITY CLASSIFICATION OF REPORT	18. SECURITY CLASSIFICATION OF THIS PAGE	19. SECURITY CLASSIFICATION OF ABSTRACT	20. LIMITATION OF ABSTRACT
Unclassified	Unclassified	Unclassified	UL

Standard Form 298 (Rev. 2-89) (EG)
Prescribed by ANSI Std. 239.18
Designed using Perform Pro, WHS/DIOR, Oct 94

Final Report on Contract F49620-03-1-0313, "Laser Cooling with Ultrafast Pulse Trains"

F.X. Kärtner and D. Kielpinski

Research Laboratory of Electronics, Massachusetts Institute of Technology

(Dated: December 7, 2005)

I. INTRODUCTION

Laser cooling and trapping are central to modern atomic physics. The low temperatures and long trapping times now routinely achieved by these means have led to great advances in precision spectroscopy and cold collision studies. These conditions also provide a suitable starting point for evaporative cooling to Bose-Einstein condensation. However, traditional laser cooling methods are easily applied only to atomic species that exhibit strong, closed transitions at wavelengths accessible by current laser technology. Only $\sim$ 20 species have been laser-cooled, mostly alkali and alkali-earth metals and the metastable states of noble gases [1].

Under contract F49620-03-1-0313, "Laser Cooling with Ultrafast Pulse Trains," we worked toward demonstrating a new method of laser cooling using the ultrafast pulses from a mode-locked laser. The mode-locked cooling method appears capable of cooling atoms that would otherwise require generation of single-frequency vacuum ultraviolet radiation, such as hydrogen and carbon [2]. Our scheme uses intense mode-locked light in the deep ultraviolet to drive two-photon scattering at high rates. Sufficient cooling forces can only be generated at high powers unavailable from single-frequency laser systems, so the high nonlinear conversion efficiency of ultrafast pulses is essential. Our method opens new atomic species to laser cooling, leading in the near term to improved spectroscopy and collision studies in hydrogen and deuterium. Furthermore, it provides a competitive route to cooling and trapping of the cold antihydrogen produced at CERN.

To test our method in a relatively simple experimental system, we chose to probe the two-photon transition of trapped Yb^+ ions at 871 nm. In this system, we have the benefit

of well-known trapping and laser cooling techniques that give us long interaction times and ultracold atomic samples, an ideal testing ground for the principles underlying the mode-locked cooling method. We constructed a Yb^+ ion trap system and successfully trapped large clouds of Yb^+ ions, laser cooling them to temperatures as low as 270 mK. We also constructed a high-repetition-rate mode-locked laser suitable for demonstrating our cooling technique and stabilized the laser carrier frequency to the $\sim$ 1 MHz level needed for laser cooling. We searched for the two-photon transition, but have not yet observed it; our theoretical predictions indicate that modest improvements to the experiment would bring mode-locked laser cooling within reach. In the course of our search, we demonstrated a new diode laser system for laser-cooling Yb^+ in the traditional manner [3]. We believe this is the shortest-wavelength laser ever directly used for laser cooling. We have also taken preliminary steps toward laser cooling of an atomic hydrogen beam. The beam source is already in place and we have begun building the laser source for optical guiding of the beam, as detailed in our original proposal for this contract.

II. TRAPPING AND DETECTING Yb^+ IONS

We constructed a linear Paul trap [4] and used it to confine Yb^+ ions (Fig. 1). The trap consists of four parallel molybdenum rods (diameter 4.75 mm) arranged in a square 6.3 mm on a side, and two molybdenum "endcap" tubes (outer diameter 2.3 mm, inner diameter 1.4 mm) protruding into the square rod arrangement with a gap of $\sim$ 20 mm between their ends. To create the trapping potential, we applied a radiofrequency (RF) voltage to the rods, amounting to a few hundred V peak-to-peak at 1 MHz, which confined the ions near the trap axis of symmetry. A DC voltage of $\geq$ 10 V applied to the endcaps provided confinement in the axial direction. Overall we estimated a trap depth of a few tens of eV.

We loaded ions into the trap by evaporating neutral Yb from an oven near the trap while a hot-filament electron gun sprayed low-energy electrons through the trapping region. Electron-impact ionization of neutral Yb inside the trapping region produced Yb^+ ions. The trap was housed in an ultra-high-vacuum (UHV) chamber with a base pressure less than 10^{-10} torr. The detection laser light passed through the two endcap tubes; a photomultiplier

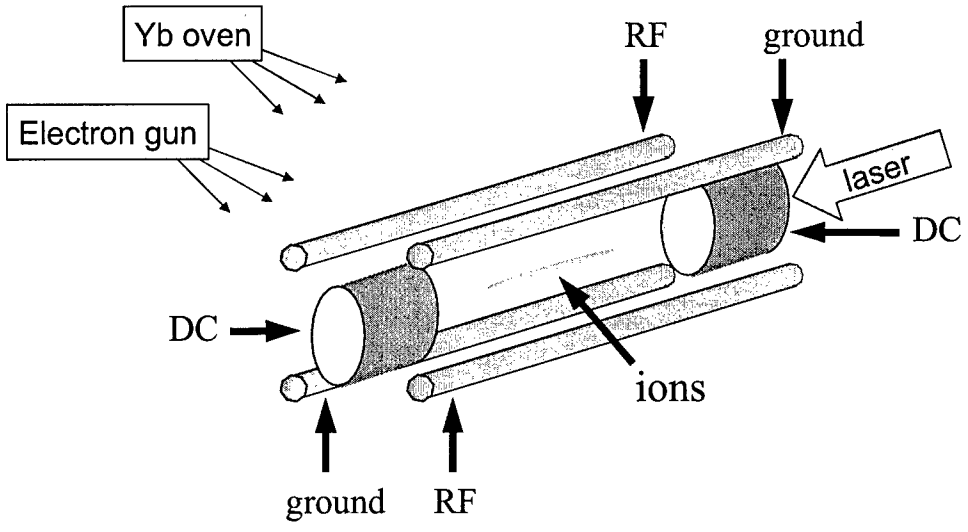

FIG. 1: Schematic of the linear RF trap. Applying RF potentials to the rod electrodes as shown generated a potential that confined ions along the axis of symmetry, while the DC potentials on the "endcap" tubes provided axial confinement. Laser light for ion excitation passed through one endcap and out the other. A photomultiplier tube (not shown) detected fluorescence collected normal to the trap axis. Neutral Yb atoms from an oven were ionized by electron impact inside the trapping region, and the resulting Yb+ ions were confined in the $\gtrsim 10$ eV trapping potential.

tube (PMT) detected the resulting fluorescence, which was collected normal to the trap axis. We could also obtain images of the ion cloud by focusing the fluorescence onto a cooled back-illuminated CCD camera. Fig. 2 shows a typical image collected over 1 s with a total of $\sim 10^4$ detected fluorescence photons.

We detected the trapped ions with narrowband 369.5 nm light, later using this light to laser cool the ions as well. The 369 nm light was resonant with the strong $S_{1/2} - P_{1/2}$ single-photon transition of the Yb^+ ion (Fig. 3). For initial experiments, we generated the light by frequency doubling of a home-built titanium:sapphire (Ti:S) ring laser operating near 739.0 nm. Later we developed a novel ultraviolet diode laser operating at a fundamental wavelength of 369.5 nm and used the laser for cooling on this transition (Sec. V, [3]). Ion fluorescence perpendicular to the trap axis was collimated with an f/1.4 plano-convex lens and refocused onto a photomultiplier tube (PMT). Stray light was blocked with an

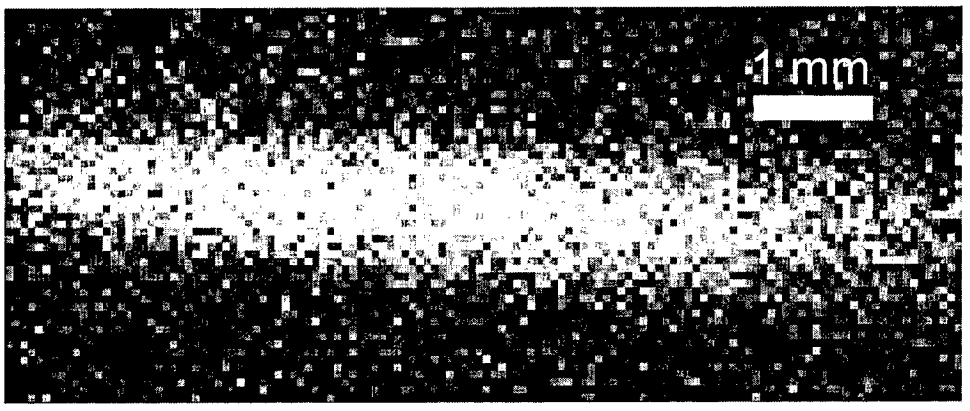

FIG. 2: A trapped cloud of Yb^+ ions, imaged by focusing 369 nm fluorescence onto a CCD camera. Integration time was 1 s.

interference filter. From the fluorescence signal size, we estimated that the trap could hold up to 10^4 – 10^5 ions. With laser cooling of smaller clouds of $\sim$ 100 ions (Sec. V), we achieved signal-to-noise ratios of 50 over 1 s integration time.

Occasionally, rather than decaying to the ground state, the excited $P_{1/2}$ state decays to the metastable $D_{3/2}$ state with lifetime 53 ms [5]. The ions can be optically pumped to the $D_{3/2}$ state under repeated excitation, leading to loss of 369 nm fluorescence. To forestall optical pumping in our initial experiments, we leaked in $\sim 10^{-6}$ mbar of nitrogen buffer gas, which collisionally relaxed metastable ions back to the ground state. Later we used another diode laser near 935.2 nm to drive the $D_{3/2}$ – $^3[3/2]_{1/2}$ "repump" transition (Fig. 3), as studied in ref. [6]. The $^3[3/2]_{1/2}$ state primarily decays to the ground $S_{1/2}$ state, returning the ion to the $S_{1/2}$ – $P_{1/2}$ scattering cycle. The 935 nm laser power was more than sufficient to drive the repump transition; under typical conditions, we could reduce the 935 nm laser power by a factor of 100 without suffering loss of signal from optical pumping.

III. MODE-LOCKED LASER CONSTRUCTION AND STABILIZATION

We constructed a high-repetition-rate mode-locked Ti:S laser suitable for testing our laser cooling technique. The requirements on this laser, in order of importance, were as

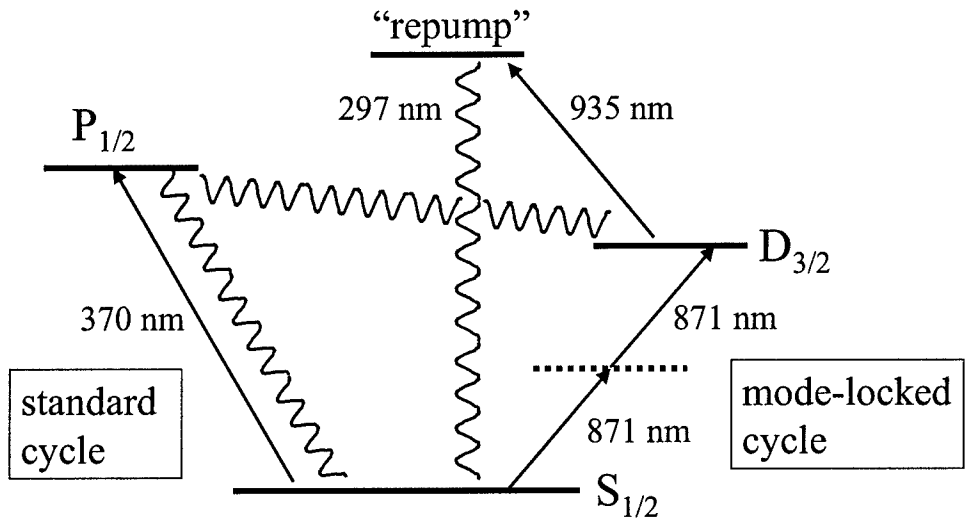

FIG. 3: Partial level scheme of the Yb^+ ion. Arrows indicate laser excitation pathways, wavy lines indicate spontaneous emission channels. The "standard" cycle consists of repeated single-photon scattering on the 369 nm transition. After scattering several thousand photons, an ion can decay to the long-lived $D_{3/2}$ state and is pumped out by the 935 nm laser. For mode-locked laser cooling, we have attempted to excite the "mode-locked" cycle (Sec. IV), in which a mode-locked laser at 871 nm excites a two-photon transition to the $D_{3/2}$ state and the 935 nm laser returns the ion to the ground state.

follows. 1) The laser must be tunable to the desired wavelength, in this case 871 nm. 2) The repetition rate must be higher than the Doppler width of the hot ion cloud, in order to resolve the Doppler shift and induce light scattering only on hot ions. Otherwise both hot and cold atoms will experience similar light forces and cooling will not occur. 3) The power of the laser must be as high as possible to maximize the two-photon scattering rate. Since each scattering event imparts a fixed momentum kick to the ion, the light force and cooling rate are directly proportional to the scattering rate. 4) The laser must emit relatively long pulses, preferably longer than 100 fs, to avoid excitation of unwanted atomic transitions and difficulties associated with dispersion management. The benefits of our laser cooling scheme come largely from the high efficiency of nonlinear frequency conversion with ultrafast lasers. Pulses as long as tens of picoseconds can have conversion efficiencies near unity, so the shortest pulses are neither necessary nor helpful for our purposes.

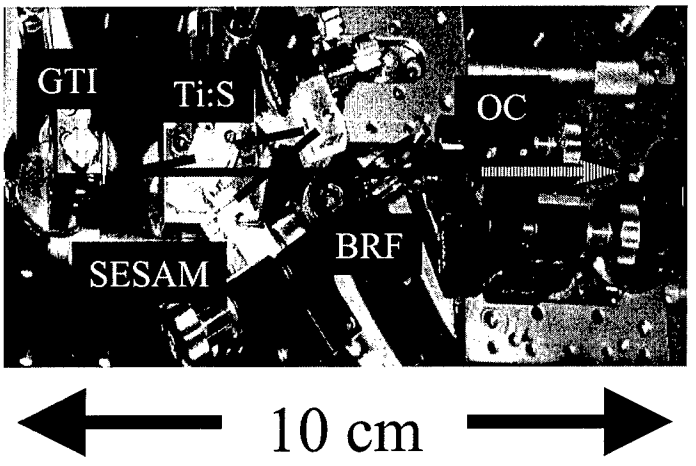

FIG. 4: The high-repetition-rate mode-locked laser, shown actual size. BRF = birefringent filter. GTI = Gires-Tournois interferometer mirror. SAM = saturable absorber mirror. Ti:S = titanium:sapphire crystal. OC = output coupler. The beam path is outlined in red. A round trip back and forth through the laser cavity is 20 cm long, providing a pulse repetition rate of 750 MHz.

The mode-locked laser is shown actual size in Fig. 4. When pumped by 10 W of 532 nm light, this laser emitted pulses of duration 260 fs at a repetition rate of 750 MHz, with an average power output of 1.2 W. The standard Kerr-lens mode-locking mechanism [7] allows only one pulse in the laser cavity at a time, requiring a cavity round-trip length of 20 cm and a very compact laser. The long (1 cm) Ti:S crystal was hydrogen-annealed to minimize infrared reabsorption, which often limits the power of Ti:S lasers [8]. The Gires-Tournois interferometer mirror provided large negative dispersion at 871 nm to cancel the material dispersion of the long crystal and allow ultrashort pulse formation. The birefringent filter provided wavelength tunability. The relatively long pulses supported by the laser did not have sufficient peak power to initiate Kerr-lens mode-locking; instead, we used a saturable absorber mirror to induce loss for CW lasing, while leaving mode-locked pulses undisturbed [9].

We stabilized the carrier frequency of the mode-locked laser frequency comb using spectroscopy of a stable Fabry-Perot interferometer (FPI), as is commonly done with CW

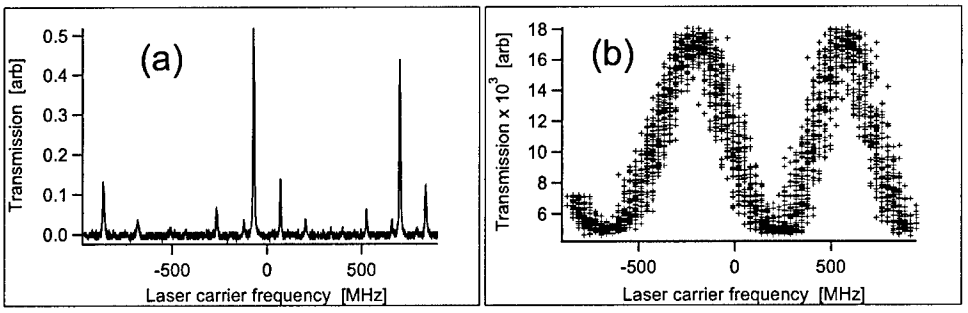

FIG. 5: Transmission spectrum of the FPI for (a) correct FPI length with $p = 1$, $q = 2$; (b) FPI length mismatched by $\sim 700\,\mu$m. The transmission signal for (a) is a factor of ~ 50 higher and narrower than for (b), and the signal-to-noise ratio is increased by a factor of ~ 2500.

lasers. An electronic error signal, generated from the FPI by the scheme of [10], was used to adjust the laser cavity length, keeping the array of mode-locked comb lines locked to the stable FPI resonances. From the residual error signal, we estimated the stabilized laser linewidth as 400 kHz over a 1 s integration time.

Because of the relatively high duty cycle of our laser, we observed temporal matching effects in the FPI optical spectrum not previously reported in the literature. These effects are best understood by considering the FPI transmission spectrum, but induce analogous effects in the error signal. The transmission spectrum of an FPI excited by a mode-locked laser shows peaks similar to those seen for a CW laser for

$$\tau_{\mathrm{FPI}} \approx \frac{p}{q}\,\tau_{\mathrm{rep}} \qquad p,\, q \text{ integers} \tag{1}$$

with τ_{FPI} the round-trip time in the FPI and τ_{rep} the time between pulses. This relation is easily understood for the case $p = q = 1$; a single pulse circulating in the FPI can interfere with an incoming pulse only if the two pulse envelopes overlap.

While we aimed for an FPI length approximately half the distance between pulses, $p = 1$, $q = 2$, we observed well-defined structure in the transmission spectrum for values of p and q as high as 200, i.e., FPI lengths within $\sim 700\,\mu$m (0.5%) of the desired length. In these cases the transmission spectrum was qualitatively similar to $p = 1$, $q = 2$ but with

smaller amplitude variation, as shown in Fig. 5. Proper temporal matching (Fig. 5a) gave a signal 50 times higher, but also 50 times narrower, than that obtained with FPI length mismatched by $\sim$ 700 μm (Fig. 5b). The signal-to-noise ratio (SNR) was $\sim$ 2500 times larger for proper matching, and the stabilized laser linewidth was inversely proportional to SNR; thus it was essential to achieve proper temporal matching. The FPI mirror curvature made it hard to compare the desired and actual FPI lengths to sub-millimeter precision, so these spurious signals initially caused some difficulty in setting up the laser stabilization.

IV. SEARCH FOR TWO-PHOTON TRANSITION

We attempted to drive the $S_{1/2}$ – $D_{3/2}$ two-photon transition at 871 nm with the mode-locked laser, as shown in Fig. 4 above. Simultaneously driving the 935 nm transition transfers ions from the long-lived $D_{3/2}$ to the high-lying repump state, which decays in 33 ns [6]. It was easy to saturate the 935 nm transition, so the resonant scattering rate on the two-photon cycle could in principle reach 1.2 MHz, given sufficient mode-locked laser power. Since this two-photon transition has not been previously studied theoretically or experimentally, we needed to predict the two-photon scattering rate ourselves, which we could do only roughly. The upper limits on the two-photon cross section that we find in the two series of experiments are within an order of magnitude of the predicted cross section, indicating that modest improvements to the apparatus would bring mode-locked laser cooling within reach.

While no calculations of two-photon cross sections in Yb^+ appear in the literature, there has been extensive theoretical and experimental work on Yb^+ single-photon transitions, leading to accurate oscillator strength values for hundreds of transitions in the DREAM database [11]. We estimate the two-photon cross section by second-order perturbation theory, using the same single-photon reduced matrix elements used to obtain the DREAM values [12]. The $6p$ intermediate configuration dominates the two-photon matrix element, and we neglect contributions from other intermediate states. For maximum repumping of the $D_{3/2}$ state and excitation with linearly polarized mode-locked light, our predicted cross section is 1.7×10^{-22} cm^4 W^{-1}, with an estimated error of a factor of two. We hesitate to

assign a smaller error to the cross section because of the breakdown of the rotating-wave approximation for our nonresonant excitation and the neglected transition amplitudes through other intermediate states.

Our primary signal of the two-photon transition was 297 nm fluorescence from the repump state, induced by simultaneous illumination with mode-locked light and 935 nm light. We searched for 297 nm fluorescence with the same optics and PMT used for detecting 369 nm fluorescence. The major difference in detection efficiency came from the transmission of the spectral filters used to block spurious detection while viewing each of the two transitions. To rule out possible experimental mishaps, we independently tested the PMT detection efficiency at the two wavelengths with a monochromator, using the sharp ultraviolet spectral lines from an Hg discharge as a reference. We also tested the transmission of the sapphire vacuum window used to collect ion fluorescence. All optics used in detecting the fluorescence had similar behavior at 369 and 297 nm. We found that, excluding the effect of filters, the detection efficiency per photon at 369 nm was 1.0 times that at 297 nm.

In our search, we (a) scanned the positions of the laser beams with respect to the ion cloud, (b) adjusted the mode-locked beam waist radius to optimize total two-photon transition rate, and (c) scanned the mode-locked laser frequency to obtain spectrally resolved data. Our search ranged widely over these parameters, and we also searched closely over a large range of each parameter while keeping all others fixed. To decrease background noise, we employed lock-in detection of the PMT signal by chopping either the mode-locked laser beam or the 935 nm laser beam at rates varying from 100 Hz to 1 kHz. Chopping the mode-locked beam should change the two-photon Rabi frequency, while chopping the 935 nm beam should change the two-photon linewidth. In either case we would expect a variation in 297 nm fluorescence. At regular intervals during the search, we measured the 369 nm fluorescence to verify that the ion number remained roughly constant.

In our first series of experiments, we used a few thousand ions at a temperature of about 3000 K (as estimated from the 369 nm Doppler width of 2.5 GHz). To achieve the maximum two-photon scattering rate, we resonantly enhanced the mode-locked light intensity at the

ions with a Fabry-Perot buildup cavity of finesse 150. The buildup cavity light passed through the same trap windows as the 369 nm light; the windows were antireflection-coated at 871 nm to minimize loss. In this way we obtained mode-locked average powers as high as 4 W. By adjusting the cavity waist radius, we varied the average intensity from 20 to 200 kW cm^{-2}. The highest intensity is sufficient to saturate the two-photon transition even for a two-photon cross section 10 times smaller than our estimated cross section (see below). Unfortunately, the small amount of 369 nm light transmitted through the buildup cavity was insufficient for single-photon laser cooling, so the spectral and spatial overlap of the ion cloud with the mode-locked light remained small. From our estimated detection efficiency and ion density, we found an upper limit of 15 KHz on the total 297 nm fluorescence rate for the whole cloud, corresponding to an upper limit on the two-photon cross section of 10^{-21} cm^4 W^{-1}.

Later we removed the buildup cavity, giving us enough 369 nm power to cool $\sim$ 100 ions to hundreds of mK (see Sec. V). The cooling improved the spectral and spatial overlap of the ions with the 369 nm light, and ought to have done the same for the mode-locked light. The mode-locked average intensity only ranged up to 10 kW cm^{-2} in these experiments, so the two-photon transition was presumably not saturated. Again we searched over parameters (a) - (c) above. In these experiments the 369 nm intensity was sufficient to saturate the response of all ions. Since the upper-state lifetime of the 369 nm transition is known, normalizing the 297 nm fluorescence signal to the saturated 369 nm signal let us deduce the two-photon scattering rate per ion without referring to estimates of detection efficiency and ion density. The higher spectral and spatial overlap roughly compensated for the reduced mode-locked light intensity, and we found an upper limit 2×10^{-22} cm^4 W^{-1} on the two-photon cross section in this case.

V. ULTRAVIOLET DIODE LASER COOLING

We used a novel ultraviolet diode laser at 369.5 nm to perform laser cooling on the $S_{1/2}$ – $P_{1/2}$ single-photon transition, achieving temperatures below 270 mK [3]. To the best of our knowledge, no shorter-wavelength laser has ever been used for laser cooling. The large

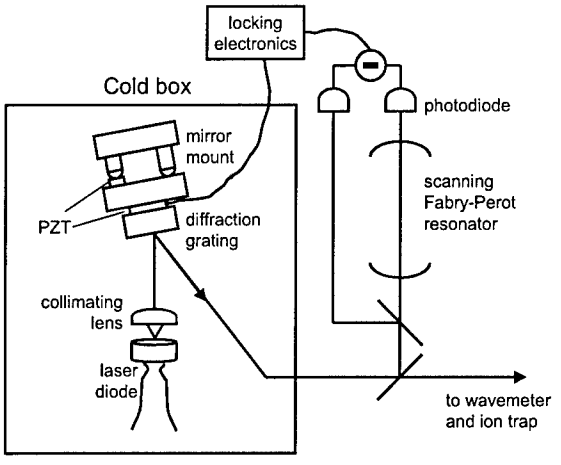

FIG. 6: Schematic of the UV laser system. A diffraction grating provides optical feedback to the UV diode in Littrow configuration. The laser cavity sits in a sealed cold box. The laser frequency is monitored and controlled by observing transmission through a scanning Fabry-Perot resonator. PZT, piezoelectric transducer.

fluorescence signals available from laser-cooled ions, a factor of 1000 greater than those observed with hot ions, will help us in future experiments on the $S_{1/2}$ – $D_{3/2}$ two-photon transition.

A schematic of the 369.5 nm laser system is shown in Fig. 6. The laser system was based on a commercial GaN laser diode (Nichia model NDHU110APAE2) with center wavelength 373 nm. With the help of Mr. P. O'Brien of MIT Lincoln Laboratory, we deposited an antireflection coating of Al_2O_3 onto the diode facet by electron-beam evaporation, resulting in a residual facet reflectivity estimated at few parts in a thousand. The coated laser diode could be wavelength-tuned by ± 1.5 nm in a Littrow-type external cavity [13]. Cooling the laser diode to $-23°C$ provided the added tuning range needed to attain stable 369.5 nm lasing with a maximum power of 400 μW.

We laser cooled clouds of $\sim$ 100 ions on the 369 nm transition. During laser cooling, we actively stabilized the frequencies of the 369 nm and 935 nm lasers to better than 1 MHz, using electronic feedback from the transmission of each laser through a Fabry-Perot resonator. The 369 nm and 935 nm lasers both saturated their respective atomic transitions.

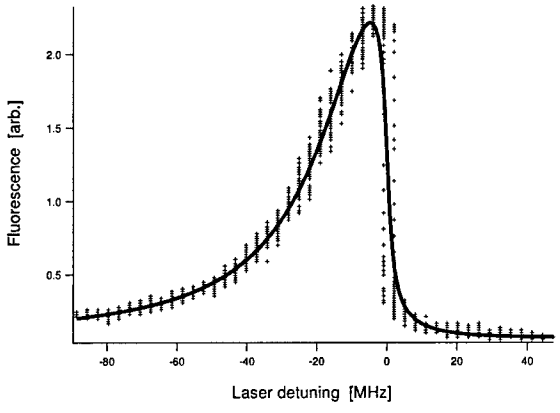

FIG. 7: Typical spectrum of cold ions. Crosses: data. Solid line: best fit to modified Voigt profile. Total linewidth was 42 MHz, mostly due to power broadening. The residual linewidth was < 23 MHz, corresponding to a temperature < 270 mK.

We scanned the 369 nm laser from the red to the blue side of the Yb^+ resonance while keeping the 935 nm laser frequency fixed, generating fluorescence spectra like that in Fig. 7. We modulated the repump laser current at 900 kHz, well above the locking bandwidth, to minimize the effect of repump laser frequency drifts.

The spectrum of Fig. 7 is typical for Doppler-cooled ion clouds in this and other experiments [14]. As the laser swept in from the red side of the Yb^+ resonance, the cloud cooled, increasing its spectral and spatial overlap with the laser, and the fluorescence signal rose dramatically. Once the ion cloud reached its minimum temperature, the overlap became more or less constant, allowing us to record a fluorescence spectrum representative of the ion temperature. Then, as the laser scanned to the blue of resonance, the ions heated rapidly and the ion fluorescence fell dramatically. Using a modified Voigt profile to fit the 369 nm spectral data gave an average atomic linewidth of 45 MHz, as compared to the natural linewidth of 19.8 MHz [15]. Most of this width came from power broadening by the high 369 nm intensity. The residual linewidth was 23 MHz, corresponding to an upper limit of 270 mK for the ion temperature.

VI. WORK TOWARD LASER COOLING OF HYDROGEN

We concentrated almost exclusively on experiments with Yb^+ ions during the grant period, owing to lack of personnel, but did take a few steps toward building up the hydrogen apparatus. We obtained and tested the single-frequency 1029 nm fiber laser and amplifier needed for the H optical dipole guide described in the original proposal. We also replaced the cryocompressor on the cryogenic H source donated by Prof. Daniel Kleppner.

We have also found a new excitation scheme for mode-locked cooling of H that maintains atomic polarization during cooling (Fig. 8), allowing us to use magnetic forces for guiding the atomic beam. In our original proposal, we suggested quenching the metastable 2S state with a DC electric field, which mixes the 2S state with the $2P_{1/2}$ state. For this cooling cycle, atoms initially polarized in the $2S_{1/2}$ $|F, m_F\rangle = |1, 1\rangle$ magnetically trapped state undergo a two-photon transition to the 2S state and are quenched through the $2P_{1/2}$ $|1, 1\rangle$ state. From that state they decay into an mixture of $2S_{1/2}$ $|1, 1\rangle$ and $|1, 0\rangle$ states through spontaneous emission. Instead we propose quenching the 2S state to the $2P_{3/2}$ $|2, 2\rangle$ state with circularly polarized microwaves at 10 GHz. This cooling cycle is closed for atoms in a stretched state, since the decay proceeds by electric dipole radiation for which m_F cannot exceed 1 (see Fig. 8). A few watts of 10 GHz power can achieve maximum quenching of the 2S state over a few cm^2. For H atoms in the 2S $|1, 1\rangle$ state, a magnetic quadrupole guide of diameter 5 mm and maximum field 1 T can produce a transverse potential well $\sim$ 50 mK deep over the 243 nm spot size of $\sim$ 100 μm. If optical guiding of the H beam is found to be infeasible, such a magnetic guide could provide an acceptable substitute.

VII. CONCLUSIONS

We have made significant progress toward a demonstration of mode-locked laser cooling using trapped Yb^+ ions. We have constructed a Yb^+ ion trap system and successfully trapped and laser-cooled clouds of Yb^+ ions. We have also constructed and frequency-stabilized a high-repetition-rate mode-locked laser appropriate for demonstrating the cooling technique. We searched for the two-photon transition, but have not yet observed

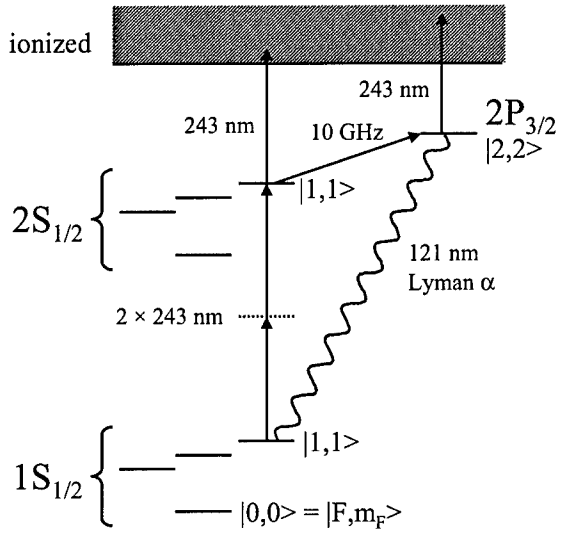

FIG. 8: Excitation scheme for laser cooling of polarized H. The 243 nm light excites the atoms from the magnetically trapped $1S_{1/2}\,|F, m_F\rangle = |1,1\rangle$ state to the $2S_{1/2}\,|1,1\rangle$ state. Radiation near 10 GHz quenches the metastable 2S state to the $2P_{3/2}\,|2,2\rangle$ state. The atoms reradiate on the $1S_{1/2}|1,1\rangle$ – $2P_{3/2}|2,2\rangle$ transition at 121 nm, returning to the magnetically trapped state. While in the $2S_{1/2}$ or $2P_{3/2}$ state, an atom can be photoionized by a single 243 nm photon. For clarity, only the relevant $2P_{3/2}$ substate is shown.

it; our theoretical predictions indicate that modest improvements to the experiment would bring mode-locked laser cooling within reach. In the course of our search, we demonstrated a new diode laser system for laser-cooling Yb^+ in the traditional manner [3]. We believe this is the shortest-wavelength laser ever directly used for laser cooling. We have also taken preliminary steps toward laser cooling of an atomic hydrogen beam. The beam source is already in place and we have begun building the laser source for optical guiding of the beam.

---

[1] H. J. Metcalf and P. van der Straten, *Laser Cooling and Trapping* (Springer, New York, 1999).

[2] D. Kielpinski, submitted to Phys. Rev. A (2005).

[3] D. Kielpinski, M. Cetina, J. Cox, and F. Kärtner, submitted to Opt. Lett. (2005), physics/0511241.

[4] M. G. Raizen et al., J. Mod. Opt. **39**, 233 (1992).

[5] N. Yu and L. Maleki, Phys. Rev. A **61**, 022507 (2000).

[6] A. S. Bell, P. Gill, H. A. Klein, A. P. Levick, C. Tamm, and D. Schnier, Phys. Rev. A **44**, 20 (1991).

[7] P. M. W. French, Contemp. Phys. **37**, 283 (1996).

[8] J. F. Pinto, L. Esterowitz, G. H. Rosenblatt, M. R. Kokta, and D. Peressini, IEEE J. Quant. Elec. **30**, 2612 (1994).

[9] F. X. Kaertner, I. Jung, and U. Keller, IEEE J. Sel. Top. Quant. Elec. **2**, 540 (1996).

[10] R. J. Jones, J.-C. Diels, J. Jasapara, and W. Rudolph, Opt. Comm. **175**, 409 (2000).

[11] E. Biémont, P. Palmeri, and P. Quinet, D.R.E.A.M.: Database on Rare Earths At Mons University, available at http://w3.umh.ac.be/ astro/dream.shtml (2005).

[12] P. Quinet, private communication (2005).

[13] G. M. Tino, L. Hollberg, A. Sasso, M. Inguscio, and M. Barsanti, Phys. Rev. Lett. **64**, 2999 (1990).

[14] L. Hornekaer and M. Drewsen, Phys. Rev. A **66**, 013412 (2002).

[15] E. H. Pinnington, G. Rieger, and J. A. Kernahan, Phys. Rev. A **56**, 2421 (1997).